Published in IET Control Theory and Applications
Received on 16th December 2011
Revised on 20th February 2013
Accepted on 21st February 2013
doi: 10.1049/iet-cta.2012.0734

ISSN 1751-8644

Output-feedback stabilisation control for a class of under-actuated mechanical systems

Liang Xu, Qinglei Hu

Department Control Science and Engineering, Harbin Institute of Technology, 150001 Harbin, People's Republic of China
E-mail: huqinglei@hit.edu.cn

Abstract: Output-feedback control of general underactuated mechanical systems is currently considered a major open problem. This study is focused on the output-feedback stabilisation control problems for a special class of underactuated mechanical systems, which appear in robotics and aerospace applications. For the synthesis of controller, first, the considered underactuated mechanical system is explicitly transformed into two cascade connected subsystems, and then an auxiliary filter-based virtual stabilisation controller is developed to locally asymptotically stabilise the first subsystem. Further, the designed virtual controller is again involved into the second subsystem using backstepping procedure to construct the actual control law, in which a series of auxiliary time-varying first-order low-pass filters are also implemented to avoid using the derivative of the system non-linear functions. Moreover, in the second step, finite-time observer technique is utilised to precisely reconstruct the immeasurable states to achieve the finite-time stabilisation control in the sense of output feedback. Lyapunov analysis shows the local asymptotic stability of the closed-loop system through the cascade system stability criteria. Simulation results are presented by using two benchmark non-linear underactuated mechanical systems to demonstrate the feasibility and the effectiveness of the proposed controller.

1 Introduction

Underactuated mechanical systems, systems with fewer inputs than degree of freedom, appear in a variety of practical plants including Robotics (e.g. flexible-link robot, non-holonomic mobile robots and walking robots), Aerospace Vehicles (e.g. helicopters, aircraft, spacecraft and satellites), underwater vehicles and surface vessels. Owing to their broad range of applications, how to control of these under-actuated systems, especially, with only output information available, has received much attention over the past decades.

The main difficulties lying in control of these underactuated mechanical systems are caused by the lack of actuation for some configuration variables. The underactuated variables can only be driven by the coupling movement of actuated variables. Besides, the existence of under-actuation would commonly admit second-order non-holonomic constraints to the mechanical systems. For these circumstances, the control problem of underactuated mechanical systems is a changeling one and open problem to be solved. Moreover today, much of the research is still focused on finding state feedback asymptotical stabilisation controllers. Few progresses have been made in the output–feedback-tracking control cases of such systems. While, the controller design for underactuated mechanical system is closely related to the controllability and accessibility analysis. Early researcher's work reveals that potential energy plays a vital role in the controllability of underactuated mechanical systems. When, certain underactuated mechanical systems, such as ground-based robot manipulators, performing tasks in potential field, they are proved to be linearisable around equilibriums and thus locally controllable. Correspondingly, the control system design is relatively easy and various control algorithms are available and have been presented for such kinds of underactuated systems, for example, energy-based control [1, 2], controlled Lagrangian [3], interconnection and damping assignment passivity-based control (IDAP) [4, 5]. However, for the underactuated mechanical systems without potential energy, the linearised system around working equilibrium is proved not to be controllable; furthermore, it can be verified that this kind of underactuated systems does not satisfy Brockett's necessary conditions, which means there exists no time-invariant and continuous control law that can asymptotically stabilise this system to its equilibrium [6]. Thus, the conventional control algorithms are ruled out in such conditions. The stabilisation for such systems might be solved with either discontinuous or time-varying control law. Different control strategies are discussed in literature, for example, sliding-mode control [7–10], motion-planning-based control [11, 12], backstepping control [13, 14], fuzzy control [15, 16]. However, these controllers are either too complicated to be adopted in practical applications or only applicable for specific systems considered. To the best of the authors' knowledge, no control algorithms are derived for a general class of underactuated mechanical systems.

Nevertheless, all of the above-mentioned results hold only for the full-state feedback control cases, and as far as we know, the problem of output-feedback control for the under-actuated mechanical systems remains open. In some under-actuated systems, the lack of actuation is usually designed

to reduce expense, size or weight, for example, underactuated industrial manipulators [17]. In those situations, velocity measurement sensors are not equipped. Furthermore, output-feedback control has the ability of avoiding the measurement noise of velocity signals. Thus, research on output-feedback control for underactuated mechanical system would be meaningful. However, just as mentioned above, owing to the complex dynamics in underactuated mechanical systems, very few results have been presented about the output-feedback control case. Only certain for specific systems are available, for example, the output-feedback control for translational oscillator with rotational actuator (TORA) system [18, 19], spherical inverted pendulum [20], mobile robot manipulator [21] and quad-rotor underactuated aerial vehicles (UAV) [22]. It should be noted that all the above-mentioned output-feedback controllers are designed for particular underactuated systems and are not applicable to other kinds of underactuated mechanical systems. In this paper, we will tackle this problem by using an auxiliary filter in a spirit similar to the recently proposed control technique in [23] for robotics and aerospace vehicles.

The main contribution is to find explicit change of coordinates and output control that transform a class of underactuated mechanical systems into cascade non-linear systems with structural properties that are convenient for control design purposes. More specifically, using the transformation and reduction technique, the underactuated mechanical system considered is firstly transformed into a cascade structure including two subsystems, and under this, an auxiliary filter is developed for designing the virtual control law for the first subsystem. Then, a new stabilisation method as stabilising non-linear output-feedback control law is introduced to the second systems. This controller is obtained via a simple recursive method like backstepping technique through a series of first-order time-varying low-pass filters that is convenient for implementation. Note that in this step a finite-time observer is involved to reconstruct the immeasurable states for finite-time stability of the closed-loop. A Lyapunov argument is used to show local asymptotical stability of the special classes of cascade underactuated systems and then the output-feedback control problem is solved explicitly. This paper is organised as follows. In Section 2, a formal problem statement accompanied by all the governing equations is presented. In Section 3, the control scheme and the associated stability analysis for the resulting closed-loop are investigated. Section 4 presents numerical simulation results, and the paper is ended with some concluding remarks in Section 5.

2 Preliminary and problem formulation

In this work, the dynamics of the mechanical systems is formulated through the Euler–Lagrange equation. The Lagrange of a simple mechanical system is the difference between a (positive semi-definite) kinetic energy and a potential energy as

$$\mathcal{L}(\boldsymbol{q}, \dot{\boldsymbol{q}}) = K - V = \frac{1}{2}\dot{\boldsymbol{q}}^{\mathrm{T}}\boldsymbol{M}(\boldsymbol{q})\dot{\boldsymbol{q}} - V(\boldsymbol{q}) \tag{1}$$

where $\boldsymbol{q} \in U$ denotes the configuration vector that belongs to an n-dimensional configuration manifold $U \subset \mathbb{R}^n$, $\boldsymbol{M}(\boldsymbol{q})$ is the positive-definite symmetric inertia matrix, K is the kinetic energy and $V(\boldsymbol{q})$ is the potential energy of the system. Then, the Euler–Lagrange equation for the mechanical system is as follows

$$\frac{\mathrm{d}}{\mathrm{d}t}\frac{\partial \mathcal{L}}{\partial \dot{\boldsymbol{q}}} - \frac{\partial \mathcal{L}}{\partial \boldsymbol{q}} = \boldsymbol{\tau} \tag{2}$$

where $\boldsymbol{\tau}$ is the generalised control inputs including either forces or torques applied on this mechanical system.

Consider the mechanical systems described by Euler–Lagrange equation in (2), two terminologies are needed in the problem formulation, that is, 'shape variable and kinematic symmetry'. Here, Shape variables-$\boldsymbol{q}_s$ are the variables that appear in the inertia matrix $\boldsymbol{M}$, that is, $\boldsymbol{M} = \boldsymbol{M}(\boldsymbol{q}_s)$, and a Lagrange system is kinetic symmetry w.r.t. q_i, if and only if the kinetic energy K of the mechanical system is invariant with respect to the configuration variable q_i, that is

$$\frac{\partial K}{\partial q_i} = 0 \tag{3}$$

In this work, the main research is restricted to a class of underactuated mechanical systems with the properties of: (i) full-actuated shape variable q_s, (ii) kinetic symmetry w.r.t q_x, and (iii) $\dot{q}_x$ does not appear in the centrifugal, Coriolis and gravity terms. When using the Euler–Lagrange expression, this special class of underactuated mechanical systems can be formulated as

$$\begin{cases} m_{xx}(q_s)\,\ddot{q}_x + m_{xs}(q_s)\,\ddot{q}_s + h_x(q, \dot{q}_s) = 0 \\ m_{sx}(q_s)\,\ddot{q}_x + m_{ss}(q_s)\,\ddot{q}_s + h_s(q, \dot{q}_s) = \tau \end{cases} \tag{4}$$

Under these conditions, the problem of output-feedback stabilisation of system in (4) is considered with only the measurement of the configuration variables (q_x, q_s).

Remark 1: The special system considered in this paper is similar to the Class I underactuated mechanical systems defined in [23]. However, compared with [23], the additional property 3) is required, which is used to extend the state-partial feedback transformation into the new cases of output-feedback.

3 Main results

3.1 Model transformation

The explicit cascade transformation to the original system is described in Lemma 1.

Lemma 1 [23]: let $\tau = \alpha(q_s)u + \beta(q, \dot{q}_s)$ be the collected partially linearising change of control for (4). Assuming all the elements of $\omega = m_{xx}^{-1}(q_s)m_{xs}(q_s)\,\mathrm{d}q_s$ are exact forms and let $\omega = \mathrm{d}\gamma(q_s)$, then there exists a global change of coordinates obtained from the Lagrangian of the system

$$\begin{aligned} q_r &= q_x + \gamma(q_s) \triangleq \Phi(q_x, q_s) \\ p_r &= m_{xx}(q_s)\,\dot{q}_x + m_{xs}(q_s)\,\dot{q}_s \end{aligned} \tag{5}$$

and transforms the dynamics of the underactuated system into a cascade normal form in strict feedback form

$$\begin{aligned} &\sum_a \begin{cases} \dot{q}_r = m_r^{-1}(q_s)p_r \\ \dot{p}_r = g_r(q_r, q_s) \end{cases} \\ &\sum_b \begin{cases} \dot{q}_s = p_s \\ \dot{p}_s = u \end{cases} \end{aligned} \tag{6}$$

doi: 10.1049/iet-cta.2012.0734

with $p_s = \dot{q}_s$ and

$$\begin{cases} m_r(q_s) = m_{xx}(q_s) \\ g_r(q_r, q_s) = -\partial V(q_r - \gamma(q_s), q_s)/\partial q_r \end{cases} \tag{7}$$

Note that the shape variable q_s can be regarded as the virtual control input for $\sum_a$-subsystem. However, it is implicitly included in unknown function $g_r(\cdot)$, which poses considerable obstacles in controller design. To linearly factor out the virtual control input q_s, the feedback change of input described by Lemma 2 is introduced.

Lemma 2 [23]: Consider the following non-linear system non-affine in control

$$\begin{cases} \dot{q}_r = N(q_s)p_r \\ \dot{p}_r = g_r(q_r, q_s) \end{cases} \tag{8}$$

where $q_r, p_r, q_s \in \mathbb{R}^n, g_r(q_r, q_s) : \mathbb{R}^n \times \mathbb{R}^n \to \mathbb{R}^n$ is a smooth function with $g_r(0,0) = 0, N(q_s)$ is a invertible matrix for all q_s, and $m_r(q_s) = N^{-1}(q_s)$ is a positive-definite and symmetric inertia matrix. Suppose there exists an isolated root $q_s = \sigma(q_r)$ of $g_r(q_r, q_s) = 0$ with the property $\sigma(0) = 0$ such that

$$\det\left(\frac{\partial g_r}{\partial q_s}(q_r, \sigma(q_r))\right) \neq 0 \tag{9}$$

and let

$$\psi(q_r, v) \triangleq [m_r(q_s)g_r(q_r, q_s)]_{q_s = \sigma(q_r)+v} \tag{10}$$

Then, for all $q_r \in \mathbb{R}^n, w = \psi(q_r, v)$ is a local diffeomorphism around a neighbourhood of $v = 0$. Assume there exists an open ball of $B_r(0)$ around $w = 0$ and a function $\varphi : \mathbb{R}^n \times \mathbb{R}^n \to \mathbb{R}^n$ such that

$$\psi(q_r, \varphi(q_r, w)) = w, \quad \forall w \in B_r(0) \subset \mathbb{R}^n \tag{11}$$

uniformly in q_r. Then the feedback change of input

$$q_s = \sigma(q_r) + \varphi(q_r, w) \tag{12}$$

transforms (8) into the following form

$$\begin{aligned} \dot{q}_r &= N(q_s)p_r \\ \dot{p}_r &= N(q_s)w \end{aligned} \tag{13}$$

It should be noted that Lemmas 1 and 2 together constitute the explicit transformation to be used in the following parts. For clarity, the following representation of coordinates is made in controller design procedures. Let

$$x_1 = q_r, \quad x_2 = p_r, \quad x_3 = q_s, \quad x_4 = p_s \tag{14}$$

Note that here only x_1, x_3 are measurable.

In view of Lemmas 1 and 2, the control task now changes to find a control law asymptotically stabilises the following cascade system with only the measurement of variables x_1 and x_3

$$\begin{aligned} &\sum_1' \begin{cases} \sum_1 & \begin{cases} \dot{x}_1 = N(x_3)x_2 \\ \dot{x}_2 = N(x_3)w \end{cases} \\ & x_3 = \sigma(x_1) + \varphi(x_1, w) \end{cases} \\ &\sum_2' \begin{cases} \sum_2 & \begin{cases} \dot{x}_3 = x_4 \\ \dot{x}_4 = u \end{cases} \\ & \tau = \alpha(x_3)u + \beta(x_1, x_3, x_4) \end{cases} \end{aligned} \tag{15}$$

Generally, input-to-state stability theorem can be employed in the controller design for cascade connected systems. However, the existence of the intermediate term $x_3 = \sigma(x_1) + \varphi(x_1, w)$ rules out its application to this paper. However, for the general cascade systems, the following lemma reveals the intrinsic stability property between cascaded subsystems, and will be used in the design and analysis of controllers for system in (15).

Lemma 3 [24]: For the cascade system

$$\begin{cases} \dot{\boldsymbol{x}} = \boldsymbol{f}(\boldsymbol{x}, \boldsymbol{z}) \\ \dot{\boldsymbol{z}} = \boldsymbol{g}(\boldsymbol{z}) \end{cases} \tag{16}$$

If $\boldsymbol{x} = \boldsymbol{0}$ is a locally asymptotically stable equilibrium of $\dot{\boldsymbol{x}} = \boldsymbol{f}(\boldsymbol{x}, \boldsymbol{0})$, and if $\dot{\boldsymbol{z}} = \boldsymbol{g}(\boldsymbol{z})$ is also locally asymptotically stable, then the composite system (16) also is locally asymptotically stable.

On the basis of Lemma 3, it can be known that if the virtual control input x_3 for $\sum_1'$-subsystem can locally asymptotically stabilise the $\sum_1'$-subsystem, and τ can also locally asymptotically stabilise the $\sum_2'$ -subsystem, then the cascade system is locally asymptotically stable. In the following parts, virtual controllers of x_3 and τ will be designed separately to achieve local asymptotical stabilisation of corresponding subsystems.

3.2 Controller design for $\sum_1'$-subsystem

In view of the above definition of variables, x_1 can be measurable, and thus if w can be designed to locally asymptotically stabilise the $\sum_1$-subsystem, then the virtual control input x_3 for $\sum_1'$-subsystem can be derived straightforwardly from $x_3 = \sigma(x_1) + \varphi(x_1, w)$. To this end, viewing work of Loria and Nijmeijer [25], the following output-feedback controller for $\sum_1$-subsystem is designed and the conclusion is stated in Theorem 1.

Lemma 4 (theorem of Barbashin *[26]*): Let $\boldsymbol{x} = \boldsymbol{0}$ be an equilibrium point of system $\dot{\boldsymbol{x}} = \boldsymbol{f}(\boldsymbol{x})$. Let $V : \mathbb{D} \to \mathbb{R}^+$ be a continuously differentiable, positive definite function on a domain D containing the origin $\boldsymbol{x} = \boldsymbol{0}$, such that $\dot{V}(x) \leq 0$ in $\mathbb{D}$. Let $S = \{x \in \mathbb{D} | \dot{V}(x) = 0\}$ and suppose that no solution can stay identically in S, other than the trivial solution $\boldsymbol{x}(t) = 0$. Then, the origin is asymptotically stable.

Theorem 1: For the subsystem

$$\sum_1 \begin{cases} \dot{x}_1 = N(x_3)x_2 \\ \dot{x}_2 = N(x_3)w \end{cases} \tag{17}$$

where $N(\cdot)$ is a positive-definite function. If the output-feedback controller is designed to be

$$\begin{aligned} w &= -k_p\tanh(x_1) - k_d\tanh(\vartheta) \\ \vartheta &= q_c + bx_1 \\ \dot{q}_c &= -a\tanh(q_c + bx_1) \end{aligned} \tag{18}$$

where a, b, k_p, k_d are positive real numbers. Then this system is asymptotically stable.

Proof: Choose the following candidate Lyapunov function for system (17)

$$V = V_1 + V_2 \tag{19}$$

where V_1, V_2 is defined respectively as

$$V_1 = \frac{1}{2}x_2^2 + k_p\ln\cosh(x_1) + \frac{k_d}{b}\ln\cosh(\vartheta) \tag{20}$$

$$V_2 = \varepsilon x_2\left(\tanh(x_1) - \tanh(\vartheta)\right) \tag{21}$$

with ε is a positive real number to be determined. To prove the positive-definite property of V, the following two auxiliary functions are considered

$$\begin{cases} W_1 = \dfrac{1}{4}x_2^2 + \dfrac{1}{4}\tanh^2(x_1)k_p + \varepsilon\tanh(x_1)x_2 \\ W_2 = \dfrac{1}{4}x_2^2 + \dfrac{1}{4}\tanh^2(\vartheta)\dfrac{k_d}{b} - \varepsilon\tanh(\vartheta)x_2 \end{cases} \tag{22}$$

It is easy to prove that $\ln|\cosh(z)| \geq \alpha\tanh^2(z)$ for all $\alpha \leq 1/2$ and for all $z \in \mathbb{R}$; therefore

$$V \geq W_1 + W_2 + \frac{1}{2}\left(k_p\ln\cosh(x_1) + \frac{k_d}{b}\ln\cosh(\vartheta)\right) \tag{23}$$

If ε is constrained to

$$\varepsilon \leq \frac{1}{2}\min\left\{\sqrt{k_p}, \sqrt{k_d/b}\right\} \tag{24}$$

Then, W_1, W_2 are positive definite. Thus, the candidate Lyapunov function V is positive definite as well. Under the designed control law (18), the closed-loop system can be rewritten as

$$\begin{cases} \dot{x}_1 = Nx_2 \\ \dot{x}_2 = N\left(-k_p\tanh(x_1) - k_d\tanh(\vartheta)\right) \\ \dot{\vartheta} = -a\tanh(\vartheta) + bNx_2 \end{cases} \tag{25}$$

Taking the derivative of (20) along trajectories (25), one can obtain

$$\begin{aligned} \dot{V}_1 &= x_2\dot{x}_2 + k_p\tanh(x_1)Nx_2 + \frac{k_d}{b}\tanh(\vartheta) \\ &\quad\times\left(-a\tanh(\vartheta) + bNx_2\right) \\ &= -\frac{ak_d}{b}\tanh^2(\vartheta) \end{aligned} \tag{26}$$

Further, the derivative of the second Lyapunov function V_2 along the trajectory of (25) can be calculated as

$$\begin{aligned} \dot{V}_2/\varepsilon &= \tanh^2(x_1)(-k_pN) + \tanh^2(\vartheta)(k_dN) \\ &\quad + x_2^2\left(\operatorname{sech}^2(x_1)N - \operatorname{sech}^2(\vartheta)bN\right) \\ &\quad + \tanh(x_1)\tanh(\vartheta)\left(k_pN + k_dN\right) \\ &\quad + \tanh(\vartheta)x_2\left(a\operatorname{sech}^2(\vartheta)\right) \end{aligned} \tag{27}$$

Thus

$$\begin{aligned} \dot{V} = \dot{V}_1 + \dot{V}_2 &= -[\tanh(x_1), \tanh(\vartheta), x_2]\,\boldsymbol{Q} \\ &\quad\times[\tanh(x_1), \tanh(\vartheta), x_2]^{\mathrm{T}} \end{aligned} \tag{28}$$

where $\boldsymbol{Q}$ is a matrix with sub-matrix as

$$\begin{aligned} \boldsymbol{Q} &= \begin{bmatrix} Q_{11} & \boldsymbol{Q}_{12} \\ \boldsymbol{Q}_{21} & \boldsymbol{Q}_{22} \end{bmatrix} \\ Q_{11} &= \varepsilon k_pN \\ \boldsymbol{Q}_{12} &= \boldsymbol{Q}_{21}^{\mathrm{T}} = \begin{bmatrix} 0.5\varepsilon(k_pN + k_dN) & 0 \end{bmatrix} \\ \boldsymbol{Q}_{22} &= \begin{bmatrix} ak_d/b - \varepsilon k_dN & 0.5\varepsilon a\operatorname{sech}^2(\vartheta) \\ 0.5\varepsilon a\operatorname{sech}^2(\vartheta) & -\varepsilon\left(\operatorname{sech}^2(x_1)N - \operatorname{sech}^2(\vartheta)bN\right) \end{bmatrix} \end{aligned} \tag{29}$$

In the following part, we will show that by appropriately choosing ε, matrix $\boldsymbol{Q}$ can be rendered positive definite.

Since $Q_{11} > 0$, based on Schur complement lemma, if one wants to set $\boldsymbol{Q} > 0$, the matrix $\boldsymbol{Q}_{22} - \boldsymbol{Q}_{12}^{\mathrm{T}}Q_{11}^{-1}\boldsymbol{Q}_{21}$ needs to be positive definite, that is

$$\boldsymbol{S} \triangleq \boldsymbol{Q}_{22} - \boldsymbol{Q}_{12}^{\mathrm{T}}\boldsymbol{Q}_{11}^{-1}\boldsymbol{Q}_{12} > 0 \tag{30}$$

where

$$\boldsymbol{S} = \begin{bmatrix} S_{11} & S_{12} \\ S_{21} & S_{22} \end{bmatrix} \tag{31}$$

The positive-definite requirement implies that all the order principal minor determinants of symmetric matrix $\boldsymbol{S}$ should be greater than zero, that is

$$S_{11} \triangleq \frac{ak_d}{b} - \varepsilon k_dN - \frac{\varepsilon N(k_p + k_d)^2}{4k_p} > 0 \tag{32}$$

$$\begin{aligned} S_{22}S_{11} - S_{12}S_{21} &= \varepsilon^2N^2\left(\operatorname{sech}^2(x_1) - b\operatorname{sech}^2(\vartheta)\right) \\ &\quad\times\left(\frac{(k_p + k_d)^2}{4k_p} + k_d\right) - \varepsilon^2\frac{a^2\operatorname{sech}^4(\vartheta)}{4} \\ &\quad -\varepsilon N\left(\operatorname{sech}^2(x_1) - b\operatorname{sech}^2(\vartheta)\right)\frac{ak_d}{b} > 0 \end{aligned} \tag{33}$$

Equation (32) implies the following constrain for ε

$$\varepsilon < \frac{4ak_dk_p}{bN(4k_dk_p + (k_p + k_d)^2)} \tag{34}$$

As for (33), define the set

$$B_\eta = \left\{x_e \triangleq [x_1, \vartheta] \in \mathbb{R}^2 : 0 < \|x_e\| < \eta\right\} \tag{35}$$

It could be observed that in the ball set B_η, $\operatorname{sech}(x_1)$, $\operatorname{sech}(\vartheta)$ are always bounded and their lower and upper bounds are represented here by positive real numbers $x_{1m}, \vartheta_m, x_{1M}, \vartheta_M$, respectively. So, if ε is sufficiently small enough and the controller parameters b is chosen to satisfy the following inequality

$$b > \frac{\operatorname{sech}^2(x_{1M})}{\operatorname{sech}^2(\vartheta_m)} \tag{36}$$

Then the following inequality would always holds in B_η (see (37) on bottom of the next page)

As the left part of this inequality converges to zero if ε is sufficiently small enough, whereas the right part of this

doi: 10.1049/iet-cta.2012.0734

inequality actually is always negative if constraint (36) is satisfied; thus (37) do always holds in B_η. Moreover, (37) actually leads to the desired results for (33).

From the above analysis, matrix $\boldsymbol{Q}$ can be made positive definite in $[x_1, \vartheta] \in B_\eta$ if sufficiently small ε is chosen and b is chosen to satisfy constrain (36). It should be noted that because ε does not appear in the control law and appears only in the stability analysis part, sufficiently small ε always exists.

Based on the above calculation, we know that by appropriately choosing the positive number ε, V can be set to be positive definite at the same time $\dot{V}$ is set to be negative definite. Thus from Lemma 4, we can infer that $\dot{V}$ will eventually converge to zero, which implies asymptotically convergence of system state x_1, ϑ, x_2. All these prove the asymptotical stability of system (17) under controller (18). This completes the proof. □

When to backstepping the virtual control law of $\sum_1$-subsystem to the $\sum_2$-subsystem, reference signal of x_3 following (15) should be given as

$$\begin{aligned} \bar{x}_3 &= \sigma(x_1) + \varphi(x_1, -k_p \tanh(x_1) - k_d \tanh(\vartheta)) \\ \vartheta &= q_c + b x_1 \\ \dot{q}_c &= -a \tanh(q_c + b x_1) \end{aligned} \tag{38}$$

Remark 2: Compared with the stability analysis procedure of Loria and Nijmeijer [24], the use of Schur complement lemma in this paper significantly simplify the stability analysis procedure and design process of the control gain.

Remark 3: The proof of Theorem 1 requires a, k_p, k_d to be positive numbers and b to satisfy (36). As long as this requirement is ensured, the existences of sufficient small positive number ε can be guaranteed to satisfy the stabilisation conditions. However, it should be noted that if we only deals with systems (17), arbitrary satisfactory positive values can be chosen for those controller parameters. However, in the context of this paper, the choice of a, b, k_p, k_d are limited to certain values to allow for the conduction of model transformation stated in Lemma 2. Thus, the value of a, b, k_p, k_d should be disposed specifically for different underactuated mechanical systems.

3.3 Controller design for $\sum_2'$-subsystem

From the above analysis, the virtual tracking signal for $\sum_2'$-subsystem is already derived as given by $\bar{x}_3$. Then, in view of backstepping design technique, $\bar{x}_3$ can be involved into the $\sum_2$-subsystem to design the control law u, and then from $\tau = \alpha(x_3)u + \beta(x_1, x_3, x_4)$, the actual control law τ can be calculated. However, this method can be directly applied to state feedback form, while, for the output-feedback case, there are two issues to be solved. The one is: the variable x_4 in $\tau = \alpha(x_3)u + \beta(x_1, x_3, x_4)$ is immeasurable, which renders the transform of input hardly feasible in output-feedback form, and the other problem is: in the backstepping design procedure, the derivative of virtual signal $\bar{x}_3$ is needed, which may require additional information of the immeasurable signal x_2.

In the following parts, the two problems are solved with finite-time observer and low-pass filter techniques. The finite-time observers are used to reconstruct the immeasurable states in finite time, which renders the input transformation $\tau = \alpha(x_3)u + \beta(x_1, x_3, x_4)$ applicable; under this, the introduction of first-order low-pass filters during each recursive step avoids the derivatives of virtual signals from the front step, and thus the output-feedback circumstances are solved totally. The detailed design procedure is shown as follows.

3.3.1 *Finite-time observer design:*

For the purpose of estimation of the unmeasured coordinate x_4, the following finite-time observer [27] is introduced

$$\begin{aligned} \dot{\hat{x}}_3 &= \hat{x}_4 + k_{o1} \left| x_3 - \hat{x}_3 \right|^{\alpha_o} \operatorname{sgn}\left(x_3 - \hat{x}_3\right) \\ \dot{\hat{x}}_4 &= u + k_{o2} \left| x_3 - \hat{x}_3 \right|^{2\alpha_o - 1} \operatorname{sgn}\left(x_3 - \hat{x}_3\right) \end{aligned} \tag{39}$$

It has been proved that if parameters are chosen to satisfy $\alpha_0 \in (0.5, 1), k_{o1}, k_{o2} \in \mathbb{R}^+$, then the observer error system is finite-time stable, which means when $t > t_s$ (t_s is the setting time for finite-time observers), the observer states equal to the system states, that is, $\hat{x}_3 = x_3, \hat{x}_4 = x_4$. For space limitation, the details of the derivative process are omitted here; see for example, [27].

To this end, the following design procedure of the controllers is assumed that states x_3 and x_4 can be reconstructed precisely in finite-time period. The design procedure is given below.

3.3.2 *Backstepping controller design for $\sum_2$-sub-system:*

Step 1: To avoid the derivative of $\bar{x}_3$ in the controller design step, an auxiliary system is introduced for the virtual input $\bar{x}_3$ by using a time-varying first-order low-pass filter, that is

$$\epsilon_3(t)\dot{x}_{3f} + x_{3f} = \bar{x}_3, \quad \bar{x}_3(0) = x_{3f}(0) \tag{40}$$

where $\epsilon_3(t)$ is a time-varying function to be designed later.

Define the following error variables

$$z_3 = x_3 - x_{3f} \tag{41}$$

The derivative of z_3 can be given as

$$\dot{z}_3 = \dot{x}_3 - \dot{x}_{3f} = x_4 - \dot{x}_{3f} \tag{42}$$

To this end, the virtual input for x_4 can be designed to be

$$\bar{x}_4 = -k_3 z_3 + \dot{x}_{3f} \tag{43}$$

with k_3 to be positive control gains.

$$\begin{aligned} &\varepsilon \left(\left(\operatorname{sech}^2(x_1) N - \operatorname{sech}^2(\vartheta) b N \right) * \left(\frac{N(k_p + k_d)^2}{4k_p} + N k_d \right) - \frac{a^2 \operatorname{sech}^4(\vartheta)}{4} \right) \\ &> \left(N \left(\operatorname{sech}^2(x_1) - b \operatorname{sech}^2(\vartheta) \right) \frac{a k_d}{b} \right) \end{aligned} \tag{37}$$

Step 2: Similarly, another auxiliary system for $\bar{x}_4$ is designed by the following low-pass filter

$$\epsilon_4(t)\dot{x}_{4f} + x_{4f} = \bar{x}_4, \quad \bar{x}_4(0) = x_{4f}(0) \tag{44}$$

where $\epsilon_4(t)$ is a time-varying function to be designed later.

Accordingly, define the following error variable z_4

$$z_4 = x_4 - x_{4f} \tag{45}$$

Then, the error dynamics can be calculated as

$$\dot{z}_4 = \dot{x}_4 - \dot{x}_{4f} = u - \dot{x}_{4f} \tag{46}$$

Then, the control input is chosen as

$$u = -k_4 z_4 + \dot{x}_{4f} \tag{47}$$

where $k_4 \in \mathbb{R}$.

In the following section, the asymptotical stability property is thoroughly analysed.

3.3.3 Stability analysis for $\sum_2$-subsystem: First, let us define the following filter error variables

$$y_3 = x_{3f} - \bar{x}_3, \quad y_4 = x_{4f} - \bar{x}_4 \tag{48}$$

From the definition of z_3 and z_4 in (40) and (44), respectively, one has

$$x_3 = z_3 + x_{3f} = z_3 + y_3 + \bar{x}_3 \tag{49}$$

$$x_4 = z_4 + x_{4f} = z_4 + y_4 + \bar{x}_4 \tag{50}$$

Further from the relations (48) and (49), the dynamics of the closed-loop system for $\sum_2$ in the form of new coordinates y_3, z_3, y_4, z_4, under control law in (46) can be formulated as

$$\sum_3 \begin{cases} \dot{z}_3 = -k_3 z_3 + z_4 + y_4 \\ \dot{z}_4 = -k_4 z_4 \\ \dot{y}_3 = -y_3/\epsilon_3(t) + B_3(x_1, x_2, \vartheta) \\ \dot{y}_4 = -y_4/\epsilon_4(t) + B_4(x_1, x_2, x_3, \vartheta) \end{cases} \tag{51}$$

where $B_3(x_1, x_2, \vartheta) = -\dot{\bar{x}}_3, B_4(x_1, x_2, x_3, \vartheta) = -\dot{\bar{x}}_4$.

It can be easily verified that the stability property of the original closed-loop system is the same as the transforms systems in (50). To analyse the stability property of $\sum_3$-subsystem, the following assumption is introduced in advance.

Assumption 1: There exist time-varying positive functions $\delta(t)$ converging to zero as $t \to 0$ and satisfying

$$\lim_{t\to\infty} \int_0^t \delta(\omega)\, \mathrm{d}\omega = \rho < \infty \quad \text{and} \quad \dot{\delta}(t) = -l(t)\delta(t)$$

with finite positive real constants ρ and functions $l(t) > 0$.

Note that there are many choices for $\delta(t)$ that satisfies the Assumption 1. For example, $e^{-l_1 t}$ with $l_1 > 0, (1+t)^{-l_2}$ with $l_2 > 1$. Then the following conclusion statement can be given:

Theorem 2: For $\sum_3$-subsystem in (50), if $\epsilon_3(t)$ and $\epsilon_4(t)$ are selected with

$$\epsilon_i(t) = \varrho_i \delta_i(t), \quad (i = 3, 4)$$
$$\varrho_3 < \frac{2}{\delta_3(0)}, \quad \varrho_4 < \frac{2}{\delta_4(0) + 1} \tag{52}$$

and $k_3 > 1, k_4 > 1/2$, then given any positive number p, for all initial conditions satisfying $(x_1^2 + x_2^2 + x_3^3 + \vartheta^2) < 2p$, the closed-loop $\sum_3$-subsystem is asymptotically stable.

Proof: Define the following Lyapunov function candidate

$$V_3 = \frac{1}{2}z_3^2 + \frac{1}{2}z_4^2 + \frac{1}{2}\delta_3(t)y_3^2 + \frac{1}{2}\delta_4(t)y_4^2 \tag{53}$$

The derivative of the Lyapunov function can be calculated as

$$\dot{V}_3 = z_3\dot{z}_3 + z_4\dot{z}_4 - \frac{l_3(t)\delta_3(t)}{2}y_3^2 + \delta_3(t)y_3\dot{y}_3 - \frac{l_4(t)\delta_4(t)}{2}y_4^2 + \delta_4(t)y_4\dot{y}_4 \tag{54}$$

Substituting system dynamics in (50) into $\dot{V}_3$, one obtains

$$\begin{aligned}\dot{V}_3 = {} & z_3(-k_3 z_3 + z_4 + y_4) + z_4(-k_4 z_4) \\ & + \delta_3(t)y_3\left(-\frac{y_3}{\epsilon_3(t)} + B_3\right) + \delta_4(t)y_4\left(-\frac{y_4}{\epsilon_4(t)} + B_4\right) \\ & - \frac{l_3(t)\delta_3(t)}{2}y_3^2 - \frac{l_4(t)\delta_4(t)}{2}y_4^2\end{aligned} \tag{55}$$

Since for any $p > 0$, the set $\Pi : (x_1^2 + x_2^2 + x_3^3 + \vartheta^2) < 2p$ is a compact set in $\mathbb{R}^4$ Therefore $\|B_i\|$ has a maximum M_i on Π.

$$\begin{aligned}\dot{V}_3 \le {} & -\left(\frac{l_3(t)\delta_3(t)}{2} + \frac{\delta_3(t)}{\epsilon_3(t)}\right)y_3^2 - \left(\frac{l_4(t)\delta_4(t)}{2} + \frac{\delta_4(t)}{\epsilon_4(t)}\right)y_4^2 \\ & + \delta_3(t)|y_3|M_3 + \delta_4(t)|y_4|M_4 - k_3 z_3^2 - k_4 z_4^2 + \frac{1}{2}z_3^2 \\ & + \frac{1}{2}z_4^2 + \frac{1}{2}z_3^2 + \frac{1}{2}y_4^2 \\ \le {} & -\left(\frac{\delta_3(t)}{\epsilon_3(t)} - \frac{\delta_3(t)}{2}\right)y_3^2 - \left(\frac{\delta_4(t)}{\epsilon_4(t)} - \frac{1}{2} - \frac{\delta_4(t)}{2}\right)y_4^2 \\ & - (k_3 - 1)z_3^2 - \left(k_4 - \frac{1}{2}\right)z_4^2 + \delta_3(t)\frac{M_3^2}{2} + \delta_4(t)\frac{M_4^2}{2}\end{aligned} \tag{56}$$

If the time-varying functions $\epsilon_3(t), \epsilon_4(t)$ are chosen to satisfy (51), then we can obtain that

$$\begin{aligned}\dot{V}_3 \le {} & -\left(\frac{1}{\varrho_3} - \frac{\delta_3(0)}{2}\right)y_3^2 - \left(\frac{1}{\varrho_4} - \frac{1 + \delta_4(0)}{2}\right)y_4^2 \\ & - (k_3 - 1)z_3^2 - \left(k_4 - \frac{1}{2}\right)z_4^2 + \delta_3(t)\frac{M_3^2}{2} + \delta_4(t)\frac{M_4^2}{2}\end{aligned} \tag{57}$$

Define

$$\boldsymbol{s} = [y_3, y_4, z_3, z_4]^{\mathrm{T}} \tag{58}$$

doi: 10.1049/iet-cta.2012.0734

and

$$\gamma = \min\left(\frac{1}{\varrho_3} - \frac{\delta_3(0)}{2}, \frac{1}{\varrho_4} - \frac{1+\delta_4(0)}{2}, k_3 - 1,\ k_4 - \frac{1}{2}\right) \tag{59}$$

Then

$$\dot{V}_3 \le -\gamma\|\boldsymbol{s}\|^2 + \delta_3(t)\frac{M_3^2}{2} + \delta_4(t)\frac{M_4^2}{2} \tag{60}$$

Integrating both sides over $[0, \infty]$ yields

$$\begin{aligned}\int_0^\infty \|\boldsymbol{s}\|^2 \mathrm{d}t &\le \frac{M_3^2}{2\gamma}\int_0^\infty \delta_3(t)\,\mathrm{d}t + \frac{M_4^2}{2\gamma}\int_0^\infty \delta_4(t)\,\mathrm{d}t \\ &\quad - \frac{(V_3(\infty) - V_3(0))}{\gamma} \\ &\le \frac{M_3^2\rho_3 + M_4^2\rho_4 + 2V_3(0)}{2\gamma} \le \infty\end{aligned} \tag{61}$$

which means $\boldsymbol{s} \in \mathcal{L}_2$. Thus, when time evolves to infinity, $\boldsymbol{s}$ converges to zero, that is

$$\lim_{t\to\infty} \|\boldsymbol{s}\| = 0 \tag{62}$$

which means the $\sum_4$-subsystem is asymptotically stable. This completes the proof. □

3.4 Stability results and further remarks

In Sections 3.2 and 3.3, the controllers are designed separately for $\sum_1'$ and $\sum_2'$-subsystem and the asymptotical stability property of the corresponding closed-loop system is thoroughly analysed. Under this, based on Lemma 3, the following results can be further concluded for the underactuated mechanical system considered in (4):

Theorem 3: Consider the system (4) with the control laws in (37) and (46). If the control gains are selected properly, the closed-loop is locally asymptotically stable in sense of output feedback, that is, $\lim_{t\to} \boldsymbol{q}(t) = 0$.

Proof: Combining Theorems 1 and 2 with Lemma 3, the proof of Theorem 3 can be given straightforwardly. □

Remark 4: The full-state feedback scheme proposed in [23] is extended to output-feedback situation via a series of constructed controllers and filters. If the estimated velocity ϑ is replaced with real one x_2, the filter gains $\epsilon_3(t), \epsilon_4(t)$ are set to be zero and the finite-time observers are removed, the proposed output-feedback controllers degrades to the full-state feedback one. This distinction is utilised in the simulation part to verify the effectiveness of the proposed controller.

Remark 5: Here the finite-time observer design satisfies the 'separation principle' such that the observer and controller can be designed separately. The only requirement for parameters of the observer is to ensure all the states of the system stay in the locally controllable domain before the setting time is arrived. If the applied controller has the ability to stabilise the system, one admissible way is to choose the observer dynamics fast enough to provide the exact evaluation of the unmeasured states. This can be easily achieved by selecting the parameters of the observer, which can be verified by simulation (see following examples).

Remark 6: From the cascade backstepping structure of the controller, it can be known that any control algorithm that can asymptotically stabilise $\sum_1$-subsystem in (15), can also be used in the recursive design procedure in $\sum_2$-subsystem to develop the control input u. Moreover, this conclusion is used in the following simulation to relax the complexity in controller designs for $\sum_1$-subsystem.

Remark 7: The closed-loop system (50) is in the form of the so-called standard singular perturbation model [25].

$$\begin{cases}\epsilon_3(t)\dot{y}_3 = -y_3 - \epsilon_3(t)\dot{\bar{x}}_3 \\ \epsilon_4(t)\dot{y}_4 = -y_4 - \epsilon_4(t)\dot{\bar{x}}_4\end{cases} \tag{63}$$

the state y_i $(i = 3, 4)$ of the fast-varying system (62), whose velocity $\dot{y}_i$ $(i = 3, 4)$ can be large when ϵ_i $(i = 3, 4)$ is small, may rapidly converge to a root of $0 = -y_i - \epsilon_i(t)\dot{\bar{x}}_i$ $(i = 3, 4)$, which is zero. In this situation, the closed-loop system dynamics of (50) is determined by the following quasi-steady-state model

$$\begin{cases}\dot{z}_3 = -k_3 z_3 + z_4 \\ \dot{z}_4 = -k_4 z_4\end{cases} \tag{64}$$

Furthermore, by appropriately choosing the parameters k_3, k_4, system (63) can be rendered stable. This singular perturbation model also implies that the reducing ϵ_i $(i = 3, 4)$ diminishes the effect y_4 in (63), which tells us that the introduction of the low-pass filters does not significantly affect the stability property of system (63).

Remark 8: At each step in backstepping procedure, an auxiliary low-pass filter is also introduced to avoid the derivative of the virtual control input. This is essentially the same strategy used in the dynamic surface control algorithm [28] to relax the computational burden caused by derivatives of nonlinear functions in intermediate virtual inputs. However, compared with conventional adaptive dynamic surface control methods introduced in [28], the design of the time-varying first-order low-pass filter renders the tracking error asymptotically converges to zero as time evolves to infinity. When referred to conventional dynamic surface control, the designed function ϵ_i $(i = 3, 4)$ could be regarded as specific constant real numbers. However, as to the proposed controller in this paper, ϵ_i $(i = 3, 4)$ changes to time-varying functions decreasing quickly towards zero, which essentially means the expanding of the bandwidth of the first-order low-pass filters. Especially, when time evolves to infinity, the low-pass filter will change to a full-pass filter, which is actually a direct-pass block. Then, the designed dynamic surface control degrades to backstepping control with the replacement of the symbolic derivative calculation to a numerical one. It should be noted that the computation burden would increase dramatically when ϵ_i $(i = 3, 4)$ becomes small enough. In this case, the compromise between computation burden and control performance should be made by deciding when to stop changing the gains of the designed first-order low-pass filters.

Remark 9: When the designed control torque is applied to the underactuated system, the closed-loop dynamics for $\sum_1'$-subsystem turns out to be

$$\sum_4 \begin{cases}\dot{x}_1 = N(z_3 + y_3 + \bar{x}_3)x_2 \\ \dot{x}_2 = g(x_1, z_3 + y_3 + \bar{x}_3)\end{cases} \tag{65}$$

The coordinates (y_3, z_3) act as a perturbation term to $\sum_4$-subsystem. If the convergence rate of (y_3, z_3) could be made faster, one would expect a better performance of $\sum_4$-subsystem. Based on this philosophy, the following calculation tries to deduce the explicit upper $\mathcal{L}_2$-norm bounds for the perturbation term (y_3, z_3).

From (56), one has

$$\dot{V}_3 \leq -\left(\frac{1}{\varrho_3} - \frac{\delta_3(0)}{2}\right) y_3^2 + \delta_3(t)\frac{M_3^2}{2} + \delta_4(t)\frac{M_4^2}{2} \tag{66}$$

Integrating both sides the above equation, one can obtain

$$\int_0^\infty y_3(\tau)^{\mathrm{T}} y_3(\tau)\,\mathrm{d}\tau \leq \frac{1}{(1/\varrho_3) - [\delta_3(0)/2]} \times \left(V_3(0) + 0.5\rho_3 M_3^2 + 0.5\rho_4 M_4^2\right) \tag{67}$$

Thus

$$\|y_3(\tau)\|_{\mathcal{L}_2}^2 \leq \frac{1}{(1/\varrho_3) - [(\delta_3(0))/2]} \times \left(V_3(0) + 0.5\rho_3 M_3^2 + 0.5\rho_4 M_4^2\right) \tag{68}$$

Similarly, one can also obtain

$$\|z_3(\tau)\|_{\mathcal{L}_2}^2 \leq \frac{1}{(1/\varrho_4) - [(1+\delta_4(0))/2]} \times \left(V_3(0) + 0.5\rho_3 M_3^2 + 0.5\rho_4 M_4^2\right) \tag{69}$$

It could be observed from (67) and (68) that the upper bounds on signals y_3 and z_3 are partially decided by ϱ_3 and ϱ_4, respectively. The smaller the ϱ_3 and ϱ_4, the smaller the values of $\|y_3\|_{\mathcal{L}_2}$ and $\|z_3\|_{\mathcal{L}_2}$ would be. Thus, we would expect a faster convergence of the errors with a smaller value of ϱ_3 and ϱ_4.

4 Simulation studies

To study the effectiveness of the proposed control strategies, the detailed response is numerically simulated with two benchmark non-linear underactuated mechanical systems, that is,. the TORA system and the inertia-wheel pendulum (IWP) system, in conjunction with the proposed control laws. Simulations comparisons are also conducted with the full-state feedback scheme signalled in Remark 4 to valid the performance of the proposed controller.

4.1 Simulations of the TORA system

The TORA system consists of a translational oscillating platform with mass m_1 which is controlled via a rotational eccentric mass m_2. Configuration of this system is depicted in the Fig. 1.

The Lagrange dynamics of the TORA system is formulated as

$$\begin{cases}(m_1+m_2)\ddot{q}_x + m_2 r\cos(q_s)\ddot{q}_s - m_2 r\sin(q_s)\dot{q}_s^2 + k_1 q_x = 0\\ m_2 r\cos(q_s)\ddot{q}_x + (m_2 r^2 + I)\ddot{q}_s + m_2 g r\sin(q_s) = \tau\end{cases} \tag{70}$$

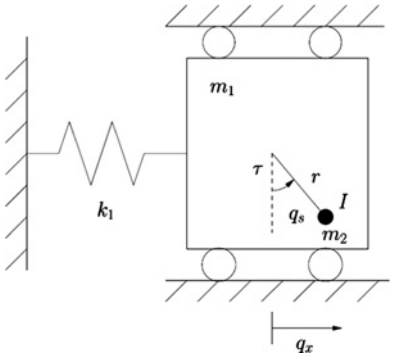

Fig. 1 *TORA system*

Table 1 Physical parameters of TORA system

Description	Parameter	Value	Units
cart mass	m_1	10	kg
arm mass	m_2	1	kg
arm eccentricity	R	1	m
arm inertia	I	1	Kg/m^2
spring stiffness	k_1	5	N m

In view of Lemma 1, the following global change of coordinates

$$\begin{cases}q_r = q_x + (m_2 r\sin(q_s))/(m_1+m_2)\\ p_r = (m_1+m_2)\dot{q}_x + m_2 r\cos(q_s)\dot{q}_s\end{cases} \tag{71}$$

would transform the dynamics of TORA system into a cascade non-linear system in strict feedback form

$$\sum\nolimits_{\text{TORA-1}} \begin{cases}\dot{x}_1 = (m_1+m_2)^{-1}\dot{x}_2\\ \dot{x}_2 = -k_1 x_1 + k_1 m_2 r\sin(x_3)/(m_1+m_2)\end{cases}$$
$$\sum\nolimits_{\text{TORA-2}} \begin{cases}\dot{x}_3 = x_4\\ \dot{x}_4 = u\end{cases} \tag{72}$$

with $x_i (i = 1, \ldots, 4)$ defined in (14).

In the simulation, the parameters for the TORA system are chosen to be the same as in [23], which is given in Table 1.

It is easy to design the virtual control law as

$$\begin{aligned}\bar{x}_3 &= -k_p\tanh(x_1) - k_d\tanh(\vartheta)\\ \vartheta &= q_c + bx_1\\ \dot{q}_c &= -a\tanh(q_c + bx_1)\end{aligned} \tag{73}$$

with

$$k_p + k_d \leq 0.5\pi \tag{74}$$

and it can asymptotically stabilise the $\sum_{\text{TORA-1}}$-subsystem to its original. Based on the conclusions drawn in Remark 5, this virtual control law can be used in the following backstepping procedure to derive the final control torque.

For the full-state feedback, the controller parameters are chosen to be: $\epsilon_3(t) = \epsilon_4(t) = 0, k_p = 0.9, k_d = 0.65,$

doi: 10.1049/iet-cta.2012.0734

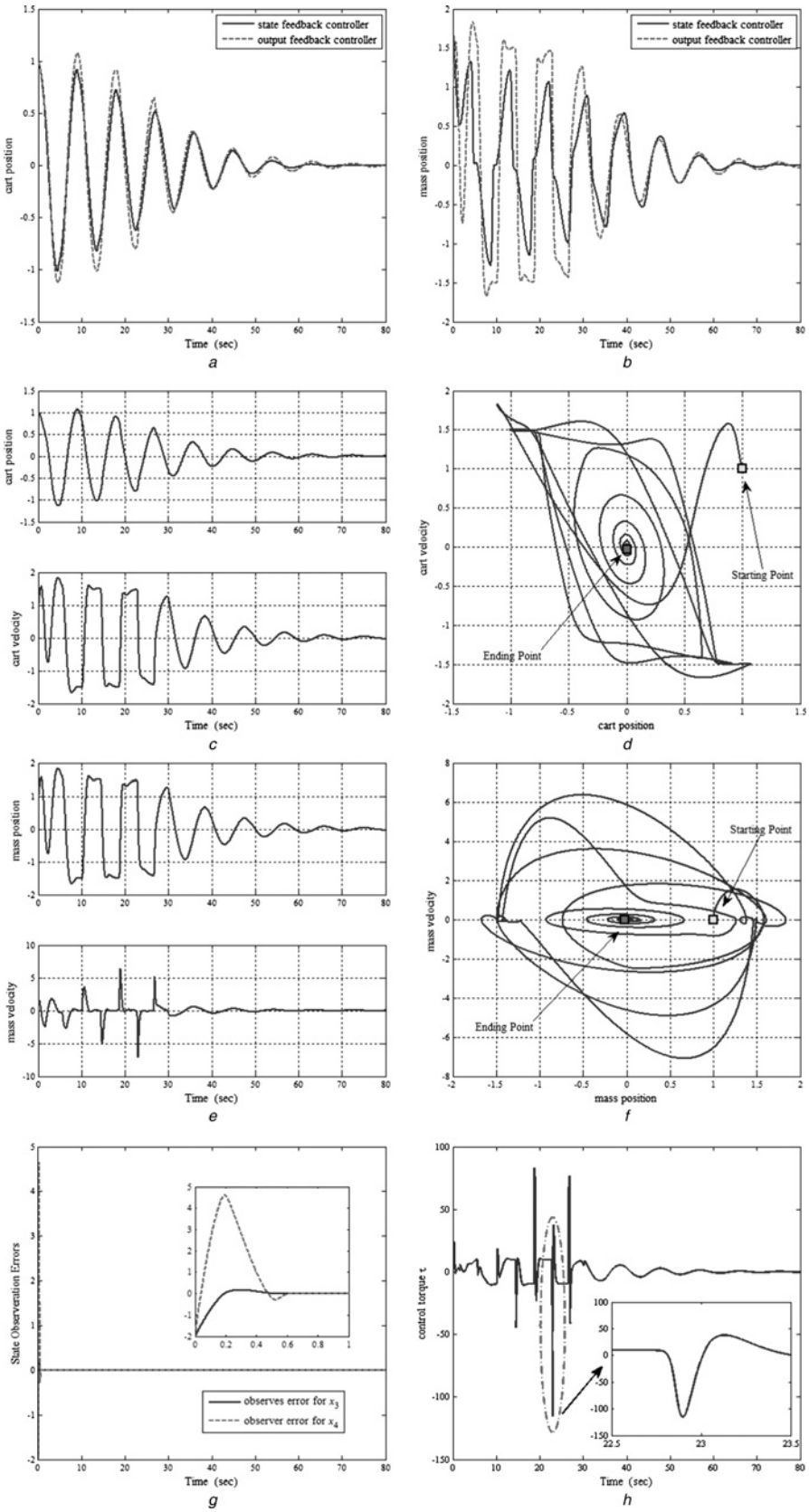

Fig. 2 *Simulated results of the TORA system*

a Full-state and output-feedback comparison – cart response
b Full-state and output-feedback comparison – eccentric mass response
c Position and velocity responses of the cart
d Phase portrait of the cart
e Position and velocity responses of the eccentric mass
f Phase portrait of the eccentric mass
g Observer errors of the designed finite-time observer
h Time response of the control torque

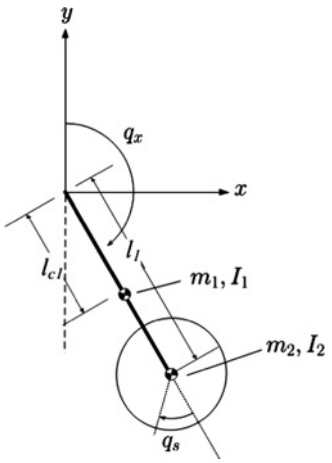

Fig. 3 *IWP system*

$k_3 = 2$ and $k_4 = 2$. The output-feedback controller parameters are chosen to be: $a = 20, b = 60, \epsilon_3(t) = \epsilon_4(t) = e^{-0.1t}$, $k_p = 0.3, k_d = 1.25, k_3 = 2$ and $k_4 = 4$, the observer gain are chosen to be $k_{o1} = 10, k_{o2} = 40$ and $\alpha_o = 0.7$. The simulation results are shown in Fig. 2.

Figs. 2*a* and *b* show the comparisons between full-state and output-feedback controllers. As it can be seen, the closed-loop trajectory with the proposed output-feedback controller shows an almost identical behaviour with the trajectory of the full-state feedback system, concluding the effectiveness of the proposed scheme. Figs. 2*c* and *d* show the responses of the cart position and velocity. It could be observed that after finite times of oscillations, the cart position and velocity converge and stay at zero. The same is also true for the response of eccentric mass shown in Figs. 2*e* and 2*f*. Fig. 2*g* shows the observer errors of the designed finite-time observer. It takes about 0.7 s for the finite-time observer to precisely reconstruct the auxiliary variables x_3 and x_4. Then after the setting time, the observer errors stay to zero permanently. Fig. 2*h* illustrates the control torque generated by the controller. Smooth control torque is generated by the proposed output-feedback controller.

4.2 Simulations of the IWP system

The inertia wheel pendulum consists of a pendulum with a rotating inertia-wheel at its end. The pendulum is unactuated and the system has to be controlled via the rotating wheel. The task is to stabilise the pendulum in its upright equilibrium point while the wheel stops rotating. The configuration of the IWP is shown in Fig. 3.

The Lagrange dynamics of this system can be formulated as

$$\begin{cases} d_{11}\ddot{q}_x + d_{12}\ddot{q}_s = \phi(q_x) \\ d_{21}\ddot{q}_x + d_{22}\ddot{q}_s = \tau \end{cases} \tag{75}$$

with

$$\begin{aligned} d_{11} &= m_1 l_{c1}^2 + m_2 l_1^2 + I_1 + I_2 \\ d_{12} &= d_{21} = d_{22} = I_2 \\ \phi(q_x) &= (m_1 l_{c1} + m_2 l_1) g \sin(q_x) \end{aligned} \tag{76}$$

where q_x is the pendulum angle, q_s is the disk angle, τ is the motor torque input.

Table 2 Physical parameters of the IWP system

Description	Parameter	Value	Units
pendulum length	l_1	0.125	m
pendulum CM	l_{c1}	0.063	m
pendulum mass	m_1	0.020	kg
wheel mass	m_2	0.300	kg
pendulum inertia	I_1	47×10^{-6}	Kg/m^2
wheel inertia	I_2	32×10^{-6}	Kg.m^2

Then from Lemma 1, we know that there exists a transformation of variable that transform the system into

$$\begin{aligned} &\sum\nolimits_{\text{IWP-1}} \begin{cases} \dot{x}_1 = d_{11}^{-1} x_2 \\ \dot{x}_2 = (m_1 l_{c1} + m_2 l_1) g \sin(x_1 - d_{12} x_3 / d_{11}) \end{cases} \\ &\sum\nolimits_{\text{IWP-2}} \begin{cases} \dot{x}_3 = x_4 \\ \dot{x}_4 = u \end{cases} \end{aligned} \tag{77}$$

In the simulation, the physical parameters of the IWP system is chosen to be the same as in [29], which gives in Table 2).

Similar to the TORA system, the asymptotic stabilisation control law for $\sum_{\text{IWP-1}}$-subsystem can be chosen as

$$\begin{cases} \bar{x}_3 = (x_1 + k_p \tanh(x_1) + k_d \tanh(\vartheta)) d_{11}/d_{12} \\ \vartheta = q_c + b x_1 \\ \dot{q}_c = -a \tanh(q_c + b x_1) \end{cases} \tag{78}$$

where

$$k_p + k_d \leq 0.5\pi \tag{79}$$

Then based on Theorem 3, we may draw the conclusion that the system could be locally asymptotically stabilised to zero.

For the full-state back, the controller parameters are chosen to be $\epsilon_3(t) = \epsilon_4(t) = 0$, $k_p = 0.25$, $k_d = 1.25$, $k_3 = 2$ and $k_4 = 2$. The output-feedback controller parameters are chosen to be, $a = 15, b = 2, \epsilon_3(t) = \epsilon_4(t) = 0.01\, e^{-0.1t}$, $k_p = 0.25, k_d = 1.25, k_3 = 20$ and $k_4 = 20$; the observer gain are chosen to be $k_{o1} = 10, k_{o2} = 20$ and $\alpha_o = 0.7$. The simulation results are shown in Fig. 4.

Figs. 4*a* and *b* show the comparisons between full-state and output-feedback controllers. As it can be seen, the closed-loop trajectory with the proposed output-feedback controller shows an almost identical behaviour with the trajectory of the full-state feedback system, concluding the effectiveness of the proposed scheme. Figs. 4*c* and *d* show the responses of the pendulum position and velocity. The pendulum position stays in the range of (−0.1 rad, 0.1 Eulerrad), which do not escape the linearly controllable area. Even though the velocity has a big ranges of (−3 rad/s, 1 rad/s), the time response of the pendulum position and velocity is still attractive for it only appears small overshot and exhibits a short setting time. Figs. 4*e* and *f* show the time responses of the rotating wheel position and velocity. It can be observed that the maximum velocity of the rotating wheel can be 300 rad/s, which appear during the starting time of the simulation. However, the time response only oscillates several times and it also has a quick setting time. Fig. 4*g* shows observer errors of the designed finite-time observer. Then setting time of observer is about 0.6s. After the setting time, the observer error turns to zero permanently. Fig. 4*h* illustrates the time response of the torque that also appears a peaking phenomenon. Then, it goes back below the bound of 0.5 Nm. All these prove the feasibility of the proposed controller.

doi: 10.1049/iet-cta.2012.0734

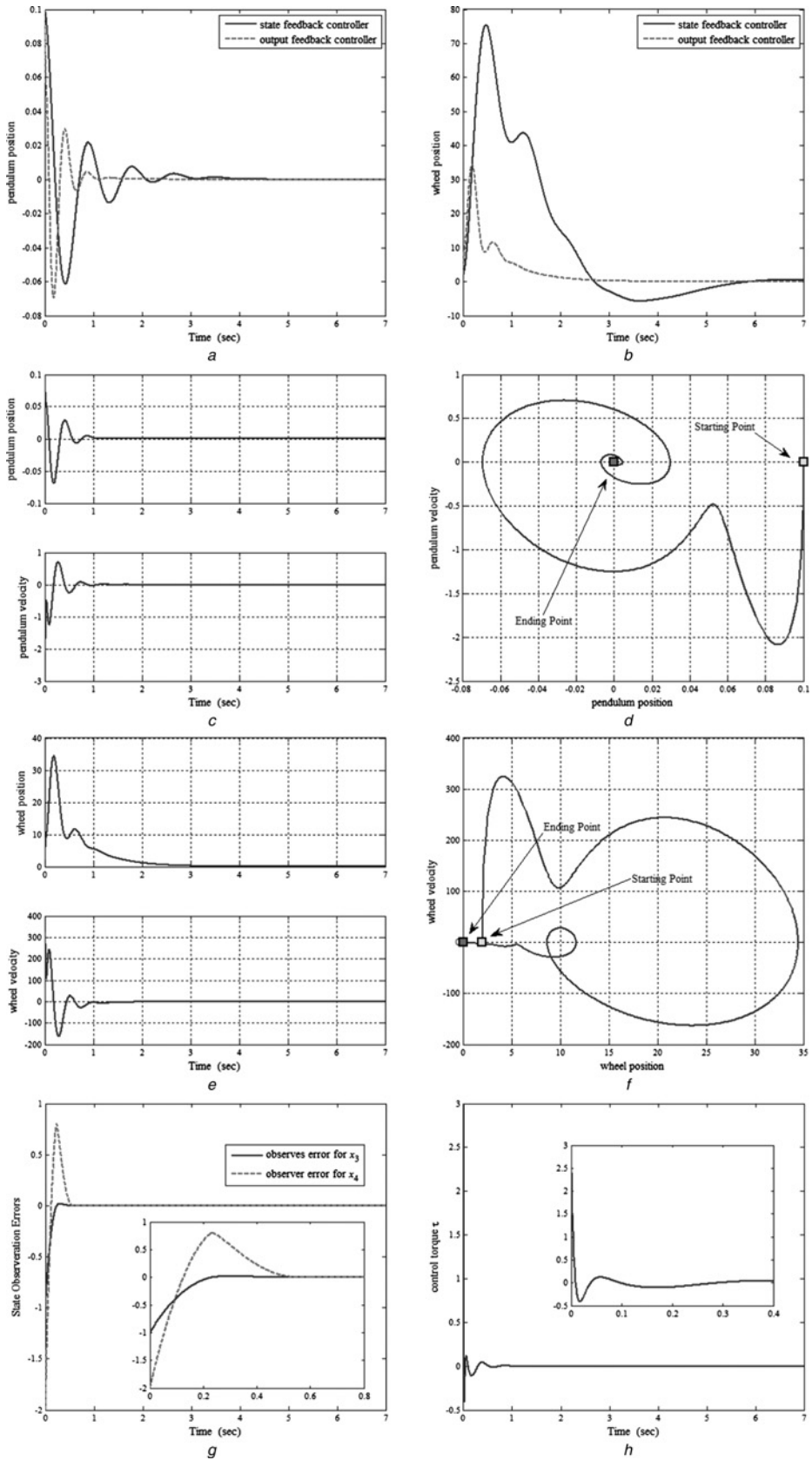

Fig. 4 *Simulated results of the IWP system*

a Full-state and output-feedback comparison – pendulum response
b Full-state and output-feedback comparison – wheel response
c Position and velocity responses of the pendulum
d Phase portrait of the pendulum
e Angle and velocity responses of the rotating wheel
f Phase portrait of the rotating wheel
g Observer errors of the designed finite-time observer
h Time response of the control torque

5 Conclusions

The output-feedback control problem for a special class of underactuated mechanical systems is investigated in this paper. The transformation and reduction technique are used for the underactuated mechanical systems to change into the cascade nonlinear systems with structural properties that are convenient for control design purposes. Then, a filter-based output-feedback controller for the changed subsystem is developed, called virtual control in sense of recursive method, and this designed virtual control is involved, like backstepping technique, into the another subsystem through a series of first-order time-varying low-pass filters to develop the actual control of the closed-loop system, in which a finite-time observer is also used to reconstruct immeasurable states. The local asymptotical stability property of the closed-loop system is analysed through the cascade system stability criteria. Simulation of two benchmark non-linear underactuated mechanical system is conducted to show the feasibility of the proposed controller. While, it should be pointed that accurate knowledge of the system dynamics is assumed to be known in advance for the control system design. Practically, because of the unavoidable uncertainties in modelling, further work is still needed for the controller design in the presence of model uncertainties.

6 Acknowledgments

This present work was supported by the National Natural Science Foundation of China (grant numbers 61004072 and 61273175), Program for New Century Excellent Talents in University (grant number NCET-11-0801), Heilongjiang Province Science Foundation for Youths (grant number QC2012C024) and the Fundamental Research Funds for the Central Universities (grant numbers HIT.NSRIF.2009003 and HIT.BRETIII.201212). The authors would also like to thank the editors and reviewers for their very constructive comments and suggestions, which have helped greatly improve the quality and presentation of the paper.

7 References

1 Sun, N., Fang, Y.C.: 'New energy analytical results for the regulation of underactuated overhead cranes: an end-effector motion-based approach', *IEEE Trans. Ind. Electron*., 2012, **59**, (12), pp. 4723–4734
2 Xin, X., Yamasaki, T.: 'Energy-based swing-up control for a remotely driven acrobot: theoretical and experimental results', *IEEE Trans. Control Syst. Technol.*, 2012, **20**, (4), pp. 1048–1056
3 Li, M.Q., Huo, W.: 'Controller design for mechanical systems with underactuation degree one based on controlled Lagrangians method', *Int. J. Control.*, 2009, **82**, (9), pp. 1747–1761
4 Ortega, R., Spong, M.W., Gomez-Estern, F., *et al.*: 'Stabilization of a class of undercactuated mechanical systems via interconnection and damping assignment', *IEEE Trans. Autom. Control.*, 2002, **47**, (8), pp. 1218–1233
5 Acosta, J.A., Ortega, R., Astolfi, A., *et al.*: 'Interconnection and damping assignment passivity-based control of mechanical systems with underactuation degree one', *IEEE Trans. Autom. Control.*, 2005, **50**, (12), pp. 1936–1955
6 Reyhanoglu, M., van der Schaft, A., McClamroch, N.H., *et al.*: 'Dynamics and control of a class of underactuated mechanical systems', *IEEE Trans. Autom. Control*., 1999, **44**, (9), pp. 1663–1671
7 Xu, R., Ozguener, U.: 'Sliding mode control of a class of underactuated systems', *Automatica*, 2008, **44**, (1), pp. 233–241
8 Sankaranarayanan, V., Mahindrakar, A.D.: 'Control of a class of underactuated mechanical systems using sliding modes', *IEEE Trans. Robot.*, 2009, **25**, (2), pp. 459–467
9 Muske, K.R., Ashrafiuon, H., Nersesov, S., *et al.*: 'Optimal sliding mode cascade control for stabilization of underactuated nonlinear systems', *J. Dyn. Syst. Meas. Control-Trans. ASME*, 2012, **134**, (2), pp. 1–11
10 Yu, R., Zhu, Q., Xia, G., *et al.*: 'Sliding mode tracking control of an underactuated surface vessel', *IET Control Theory Appl*., 2012, **6**, (3), pp. 461–466
11 Meza-Sanchez, I.M., Aguilar, L.T., Shiriaev, A., *et al.*: 'Periodic motion planning and nonlinear H-infinity tracking control of a 3-DOF underactuated helicopter', *Int. J. Syst. Sci*., 2011, **42**, (5), pp. 829–838
12 Fang, Y.C., Ma, B.J., Wang, P.C., *et al.*: 'A motion planning-based adaptive control method for an underactuated crane system', *IEEE Trans. Control Syst. Technol.*, 2012, **20**, (1), pp. 241–248
13 Chen, Y.F., Huang, A.C.: 'Controller design for a class of underactuated mechanical systems', *IET Control Theory Appl*., 2012, **6**, (1), pp. 103–110
14 Liu, Z., Yu, R., Zhu, Q.: 'Asymptotic backstepping stabilization of an underactuated surface vessel (vol 14, pg 1150, 2006)', *IEEE Trans. Control Syst. Technol*., 2012, **20**, (1), pp. 286–288
15 Hwang, C.-L., Wu, H.-M., Shih, C.-L.: 'Fuzzy sliding-mode underactuated control for autonomous dynamic balance of an electrical bicycle', *IEEE Trans. Control Syst. Technol*., 2009, **17**, (3), pp. 658–670
16 Chang, Y.-H., Chan, W.-S., Chang, C.-W., *et al.*: 'Adaptive fuzzy dynamic surface control for ball and beam system', *Int. J. Fuzzy Syst.*, 2011, **13**, (1), pp. 1–7
17 Roy, B., Asada, H.H.: 'Nonlinear feedback control of a gravity-assisted underactuated manipulator with application to aircraft assembly', *IEEE Trans. Robot.*, 2009, **25**, (5), pp. 1125–1133
18 Jiang, Z.P., Kanellakopoulos, I.: 'Global output-feedback tracking for a benchmark nonlinear system', *IEEE Trans. Autom. Control*., 2000, **45**, (5), pp. 1023–1027
19 Karagiannis, D., Jiang, Z.P., Ortega, R., *et al.*: 'Output-feedback stabilization of a class of uncertain non-minimum-phase nonlinear systems', *Automatica*, 2005, **41**, (9), pp. 1609–1615
20 Liu, G.Y., Nesic, D., Mareels, I.: 'Non-linear stable inversion-based output tracking control for a spherical inverted pendulum', *Int. J. Control*, 2008, **81**, (1), pp. 116–133
21 Li, Z.J., Yang, Y.P., Li, J.X.: 'Adaptive motion/force control of mobile under-actuated manipulators with dynamics uncertainties by dynamic coupling and output feedback', *IEEE Trans. Control Syst. Technol.*, 2010, **18**, (5), pp. 1068–1079
22 Dierks, T., Jagannathan, S.: 'Output feedback control of a quadrotor UAV using neural networks', *IEEE Trans. Neural Netw*., 2010, **21**, (1), pp. 50–66
23 Olfati-Saber, R.: 'Nonlinear control of underactuated mechanical systems with application to robotics and aerospace vehicles' (Massachusetts Institute of Technology, Massachusetts, USA, 2000)
24 Sontag, E.D.: 'Further facts about input to state stabilization', *IEEE Trans. Autom. Control*, 1990, **35**, (4), pp. 473–476
25 Loria, A., Nijmeijer, H.: 'Bounded output feedback tracking control of fully actuated Euler–Lagrange systems', *Syst. Control Lett.*, 1998, **33**, (3), pp. 151–161
26 Khalil, H.K.: 'Nonlinear Systems' (Englewood Cliffs, Prentice-Hall, NJ, 2002, 3rd edn.)
27 Perruquetti, W., Floquet, T., Moulay, E.: 'Finite-time observers: application to secure communication', *IEEE Trans. Autom. Control*, 2008, **53**, (1), pp. 356–360
28 Yip, P.P., Hedrick, J.K.: 'Adaptive dynamic surface control: a simplified algorithm for adaptive backstepping control of nonlinear systems', *Int. J. Control*, 1998, **71**, (5), pp. 959–979
29 Spong, M.W., Corke, P., Lozano, R.: 'Nonlinear control of the reaction wheel pendulum', *Automatica*, 2001, **37**, (11), pp. 1845–1851

doi: 10.1049/iet-cta.2012.0734